

Long-Range Elastic Interactions and Staging in Graphite Intercalation Compounds

S. A. Safran and D. R. Hamann

Bell Laboratories, Murray Hill, New Jersey 07974

(Received 7 March 1979)

We investigate the effects of elastic coherency strains in graphite intercalation compounds. The long-range interaction energies of two-dimensional islands of intercalant are calculated. Using the domain model of Daumas and Hérold, we show that these strains drive a mixed-stage or randomly staged crystal to pure-stage ordering.

Graphite intercalation compounds are characterized by an order sequence of n carbon and one intercalant layer, with n defining the "stage" of the material.¹ Staged compounds with c -axis periodicities of ≥ 40 Å (stage-11 FeCl₃) have recently been reported.² However, no theory for the microscopic origin of the intercalant-intercalant interactions responsible for staging has as yet been formulated. In this paper we suggest an elastic mechanism for staging based on the domain model of graphite intercalation compounds first proposed by Daumas and Hérold³ and recently discussed by Schoppen *et al.*⁴ and by Clarke, Caswell, and Solin.⁵ We calculate the interaction energy of finite-size, two-dimensional islands of intercalant³⁻⁵ which interact through the coherency strains^{6,7} which they introduce in the graphite lattice. This interaction is shown to be long ranged in that it is logarithmically dependent on z for $a_0 \gg z$, where a_0 is the island radius and z is the c -axis separation of the two islands. Although the completely ordered state ("pure-stage" material) is shown to be free of these long-range coherency strains, we show that in the mixed-stage compounds which occur during the growth, these strains do exist and drive a mixed or randomly staged compound to pure-stage ordering.

Although some workers have suggested that electrostatic⁸ or charge-density wave⁹ effects are responsible for staging, recent experimental^{10,11} and theoretical¹² evidence indicates that the electrons or holes donated to the graphite by the intercalant are mostly localized in the graphite layers which bound the intercalant. On the other hand, the elastic model discussed here requires only short-range electronic interactions and is equally applicable to both acceptors and donors. Such elastic interactions have been shown to lead to the "gas-liquid" transition of hydrogen dissolved in metals.^{7,13} However, in contrast to the calculations of the "macroscopic modes" of hydrogen in metals,¹⁴ our calculations are for intercalant islands whose dimensions are much smaller than the graphite sample size. We thus neglect the

boundary conditions at the graphite sample surface^{13,14} and calculate the elastic interactions using the infinite-medium Green's function.^{15,16}

In an infinite medium, the elastic interaction between two nonoverlapping clusters of impurities or defects with densities $\rho_1(\vec{x}')$ and $\rho_2(\vec{x})$ is given by^{6,7,13}

$$H = - \int d^3x d^3x' \rho_1(\vec{x}) W(\vec{x}, \vec{x}') \rho_2(\vec{x}'), \quad (1)$$

where $W(\vec{x}, \vec{x}')$ is related to derivatives of the Green's function,⁶ $G_{ij}(\vec{x}, \vec{x}')$, which satisfies the equilibrium equation^{6,7}

$$C_{ijkl} \frac{\partial}{\partial x_i} \frac{\partial}{\partial x_j} G_{km}(\vec{x}, \vec{x}') + \delta_{i,m} \delta(\vec{x} - \vec{x}') = 0. \quad (2)$$

In Eq. (2) C_{ijkl} is the elastic stiffness tensor, whose values for graphite are given by Seldin.¹⁷ Since we are interested in long-range interactions, we use continuum elastic theory in the linear approximation. The Green's function, $G_{ij}(\vec{x}, \vec{x}')$, is the i th component of the displacement of the elastic medium at point \vec{x} due to the j th component of a point force of strength unity, located at \vec{x}' . In our analysis, each intercalant atom is represented by a couple of forces with zero moment⁶ which further separate the graphite layers, originally separated by $c_0 = 3.35$ Å. These elastic dipoles^{6,7,13} are thus characterized by a dipole tensor $P_{\alpha\beta} = P \delta_{\alpha,\beta} \delta_{\beta,z}$.

Figure 1(a) illustrates the nature of these dipoles; two elementary dipoles in position A repel each other, while those in position B attract. For a highly anisotropic ($C_{11} > C_{33}$) medium such as graphite, the interaction energy can be calculated from Eq. (1) with^{6,7,15,16}

$$W(\vec{x}, \vec{x}') \simeq P^2 \frac{\partial^2}{\partial z^2} \left[\frac{1}{4\pi C_{44}} \frac{1}{(a_3 \rho^2 + z^2)^{1/2}} \right], \quad (3)$$

where $a_3 \simeq C_{33}/C_{44} \simeq 9$, $\rho^2 = (\vec{x} - \vec{x}')^2 + (\vec{y} - \vec{y}')^2$, and $\vec{z} = \vec{z} - \vec{z}'$. The interaction energy of two point di-

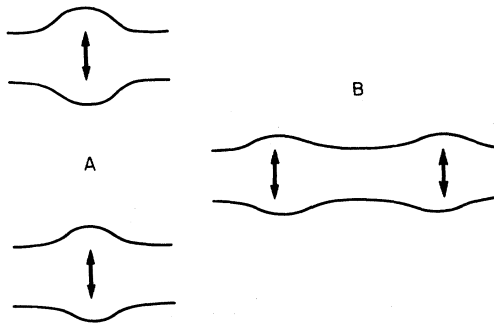


FIG. 1. Pairs of elastic dipoles (arrows) in an infinite, anisotropic medium. The dipoles in configuration A repel while those in configuration B attract.

poles is thus given by

$$H = -\frac{P^2}{4\pi C_{44}} \left[\frac{a_3 \rho^2 - 2z^2}{(a_3 \rho^2 + z^2)^{5/2}} \right]. \quad (4)$$

This interaction is attractive for $\rho > (2/a_3)^{1/2}z$ and repulsive for $\rho < (2/a_3)^{1/2}z$. Thus, the formation of intercalant islands, lying between the same two planes of graphite (configuration B), results in a lowering of the elastic energy per intercalant atom by an amount

$$\Delta U_{\text{is1}} \simeq -U_0 a_3^{-1/2} c_0 / r_0, \quad (5)$$

where $U_0 = P^2 \sigma / 2C_{33} c_0$, σ is the island density (intercalant atoms/area) and r_0 is a core cutoff length, roughly equal to the average separation of the intercalant atoms. Typical experimental values for P for hydrogen in metals are $P \simeq 3.3$ eV,¹³ so that for intercalation compounds with chemical formula $C_{6n}I$, we estimate $\Delta U_{\text{is1}} \simeq -0.13$ eV per intercalant atom.¹⁸ For small intercalant atoms such as Li, similar values for P can be obtained from calculations of the local c -axis lattice expansion. For large intercalant atoms, a description of the local distortion is beyond the range of linear elastic theory. However, the long-range strain fields considered here should still be properly described if an appropriately re-normalized effective dipole is used.

If these islands are stacked in a periodic array as shown in Fig. 2(a), they exhibit a net repulsive interaction. We first consider the interaction of two intercalant disks [e.g., A and A' in Fig. 2(a)]. Neglecting self-energy terms, we find that the interaction energy of the two disks is repulsive

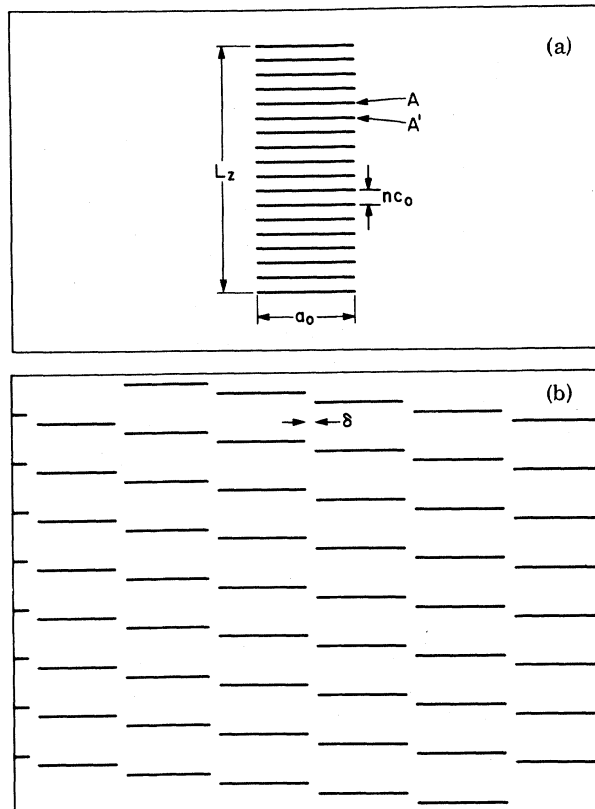


FIG. 2. (a) A single stack of intercalant islands in an infinite medium. The islands, of radius a_0 , are stacked in a periodic (staged) array of coherence length $L_z \gg a_0$, and are separated by nc_0 . A pair of such islands is denoted by A and A'. (b) A periodic array of intercalant stacks representing the domain configuration of a pure-stage crystal. The distance between intercalant islands (δ) is assumed to be much smaller than the island size a_0 .

and is given by

$$H \simeq 2W_0 \ln(24a_0/z), \quad a_0 \gg z, \quad (6a)$$

$$H \simeq W_0 a_3^{3/2} \pi (a_0/z)^3, \quad a_0 \ll z, \quad (6b)$$

where $W_0 = U_0 a_3^{-1/2} \sigma c_0 a_0$. Although for $a_0 \gg z$ the interaction energy per particle tends to zero as a_0 goes to ∞ , Eq. (6a) represents a long-range (range $z \sim a_0$) interaction between the intercalant islands. The logarithmic dependence on z is a result familiar from dislocation theory.¹⁹ Because of the long-range nature of the interaction, one must consider carefully the interactions of a disk with all the others in order to calculate the total energy. For the configuration of Fig. 2(a), a single stack in an infinite graphite medium, the energy per intercalate atom is given by $\Delta U = U_0/n$. Using the values for P and σ discussed above,

we find $\Delta U \approx 0.5 \text{ eV}/n$.

The significance of this result is that the sum of the long-range interactions of Eq. (6) results in an energy per particle which is independent of a_0 if $L_z \gg a_0 \gg nc_0$. The physical origin of this repulsive interaction is the strain induced in the graphite layers which reduce their c -axis spacing in between the intercalant layers, in order to be coherent with the rest of the sample.²⁰ One can therefore see that in a sample loaded with a periodic array of such stacks [Fig. 2(b)], these coherency strains vanish (except for edge interactions). However, in materials containing mixtures of stage- n - and stage- n' -type stacks there exists a net elastic repulsive energy. The energy per intercalant to add a single stage- n -type stack in an otherwise pure-stage- n' crystal is given by²⁰

$$\Delta U = U_0 n(1/n - 1/n')^2. \quad (7)$$

Thus, for a fixed concentration of intercalant per layer (see below) a pure-stage configuration has lower internal energy than a random- (over a distance $z \sim a_0$) or a mixed-stage crystal. For a random arrangement of islands, the strain energies (per intercalant) are independent of the island size, while the configurational entropy (per intercalant) of a random distribution of islands within a layer vanishes as $a_0 \rightarrow \infty$. Therefore the free energy is dominated by the internal energy which drives the system to a pure staged configuration.

The assumption of an equal concentration of intercalant per graphite layer is consistent with the proposed domain structure of an intercalation compound.³⁻⁵ Although this [Fig. 2(b)] configuration results in localized distortions at the island edges,²¹ these domains are stabilized by the constraint of equal concentration of intercalant per layer. This constraint is imposed by the kinetics of the intercalation process since diffusion between graphite layers is highly improbable.^{3,4}

The kinetics of the intercalation process (especially its stage dependence) should also be determined by the strain interactions discussed above. Recent experiments¹¹ indicate that during intercalation the crystal passes through all stages $n > n_0$ before reaching the final equilibrium stage of n_0 . The rate of approach to equilibrium—a pure stage—where the coherency strains vanish, depends on the elastic interactions in the mixed phases. In this paper we have calculated the repulsive elastic interactions which exist in mixed-stage materials and have shown how these inter-

actions drive the system toward pure stages. Further experimental measurements of domain sizes and ordering²² in both equilibrium and non-equilibrium states, as well as a further theoretical examination of the Hérold model, should elucidate the physics of the intercalation process.

The authors are grateful for useful discussions with F. J. Di Salvo, P. A. Lee, and T. M. Rice.

¹For general reviews, see J. E. Fischer and T. E. Thompson, *Phys. Today* **31**, 36 (1978), and to be published.

²C. Underhill, S. Y. Leung, G. Dresselhaus, and M. S. Dresselhaus, to be published.

³N. Daumas and A. Hérold, *C. R. Acad. Sci.* **268**, 373 (1969).

⁴G. Schoppen, H. Meyer-Spasche, L. Siemsglüss, and W. Metz, *Mater. Sci. Eng.* **31**, 115 (1977).

⁵R. Clarke, N. Caswell, and S. A. Solin, *Phys. Rev. Lett.* **42**, 61 (1979).

⁶R. Siems, *Phys. Status Solidi* **30**, 645 (1968).

⁷H. Wagner and H. Horner, *Adv. Phys.* **23**, 587 (1974).

⁸F. J. Salzano and S. Aronson, *J. Chem. Phys.* **44**, 4320 (1965).

⁹D. A. Young, *Carbon* **15**, 373 (1977).

¹⁰F. Batallan, J. Bok, I. Rosenman, and J. Melin, *Phys. Rev. Lett.* **41**, 330 (1978).

¹¹C. C. Shieh, R. L. Schmidt, and J. E. Fischer, to be published.

¹²L. Pietronero, S. Strässler, H. R. Zeller, and M. J. Rice, *Phys. Rev. Lett.* **41**, 763 (1978).

¹³H. Wagner, in *Hydrogen in Metals*, edited by G. Alefield and J. Völkl (Springer, Berlin, 1978), Vol. I, p. 5.

¹⁴In an infinite isotropic medium, there is no pairwise interaction between two centers of dilation (see Ref. 13). Since the elastic interactions in such systems are due to the presence of boundary conditions at the sample surface, the density modes are "macroscopic" (range of the order of the sample size) and sample shape dependent (Ref. 13). This is not the case in our calculations of the interactions of islands in a highly anisotropic medium. The density modes of interest involve intercalant islands whose sizes are assumed to be small compared with the sample size, and which interact even in an infinite medium. For macroscopic observations of strains in graphite intercalation compounds, see J. G. Hooley, *Mater. Sci. Eng.* **31**, 17 (1977).

¹⁵E. Kröner, *Z. Phys.* **136**, 402 (1953).

¹⁶J. R. Willis, *Quart. J. Mech. Appl. Math.* **18**, 419 (1965).

¹⁷O. L. Blakslee, D. G. Proctor, E. J. Seldin, G. B. Stence, and T. Weng, *J. Appl. Phys.* **41**, 3373 (1970).

¹⁸If the complete Green's function (Ref. 15) is used instead of Eq. (3), $\Delta U_{1s1} \approx -0.07 \text{ eV}$, while all our other results change by $\leq 1\%$.

¹⁹C. Kittel, *Introduction to Solid State Physics* (Wiley, New York, 1971), 4th ed., p. 679.

²⁰These coherency strains can also be relieved by the formation of misfit dislocations resulting in an *incoherent* crystal. However, it seems clear that such a disruption of the strong in-plane carbon-carbon bonds would severely hinder the observed (Refs. 3-5 and 11) smooth progression of stages and the reversibility of

the staging process.

²¹The energy per intercalant of these distortions tends to zero as $a_0 \rightarrow \infty$.

²²For a discussion of stage disorder and its dependence on the kinetics of intercalation, see W. Metz and D. Hohlwein, *Carbon* **13**, 87 (1975).

Tunneling Modes and Local Structural Order in Amorphous Arsenic

G. E. Jellison, Jr.

Solid State Division, Oak Ridge National Laboratory, Oak Ridge, Tennessee 37830

and

Gary L. Petersen

Matec, Incorporated, Warwick, Rhode Island 02886

and

P. C. Taylor

U. S. Naval Research Laboratory, Washington, D. C. 20375

(Received 5 February 1979)

Pulsed nuclear-quadrupole-resonance (NQR) measurements have been performed in rhombohedral, orthorhombic, and amorphous (*a*-) arsenic. Measurements of T_1 provide evidence of low-frequency disorder modes in *a*-As, while the NQR frequencies indicate that the bonding is predominately *p*-like in all three materials. The asymmetric NQR line shape of *a*-As indicates that bond-angle distributions inferred from x-ray scattering and continuous-random-network models do not result primarily from a distribution in bond hybridizations.

Amorphous arsenic (*a*-As) is of interest as a prototype amorphous solid because it is an elemental material and therefore should be easier to understand than chemically more complex amorphous solids. Because all of the atoms in *a*-As are threefold coordinated, this amorphous semiconductor is structurally intermediate between the tetrahedrally coordinated group-IV amorphous films (*a*-Si and *a*-Ge) and the chalcogenide glasses, which contain group-VI elements (S, Se, and Te) in twofold coordination. All chalcogenide glasses possess anomalous low-temperature thermal properties which are a manifestation of the disorder (tunneling) modes characteristic of the amorphous phase. This behavior has not been observed in *a*-As,^{1,2} which has led to the suggestion that these modes do not exist in amorphous materials which are exclusively threefold coordinated.^{1,3}

In this Letter we describe ⁷⁵As pulsed nuclear-quadrupole-resonance (NQR) measurements on *a*-As which provide the first evidence for disorder (tunneling) modes in this prototype group-V amorphous solid. The NQR also provides an extreme-

ly sensitive probe of *s-p* hybridization of the bonding electrons in the valence band. In addition, we present the first experimental evidence of the second-nearest-neighbor angular correlations implicit in the continuous-random-network (CRN) models^{4,5} of *a*-As.

There are two crystalline forms of As: the common semimetallic rhombohedral form (rh-As) and the rarer semiconducting orthorhombic form (or-As). In both crystalline forms all the atoms are threefold coordinated and form six-membered rings stacked together in a layered configuration. The NQR results of these two crystalline forms provide a useful framework for the understanding of the *a*-As data.

The pulsed NQR experiments were performed using a Matec gated pulsed amplifier and receiver in conjunction with a suitably designed matching network; the spectrometer operated between 20 and 140 MHz with a bandwidth of ~1 MHz. Variable temperatures (4-300 K) were obtained with a gas (nitrogen or helium) flow system. Typical 90°-180° pulse widths employed were approximately 10-20 μ sec. All observed decays were